Regional variation of biomechanical properties in ectatic eyes (preliminary results)

Daniela Oehring[1], Nabil Habib[2], Hetal Buckhurst[1]
1 Eye and Vision Research Group, School of Health and Human Sciences, Plymouth University, Plymouth, UK; 2 School of Optometry & Vision Sciences, Cardiff University, UK

Introduction

Keratoconus is an irreversible ocular disease (Chopra and Jain, 2005, Zadnik et al., 2002), resulting from localised stromal thinning and conical protrusion (ectasia) of the cornea. The thinning occurs mostly at the lower temporal cornea, but also at the central (Auffarth et al., 2000) and superior regions (Prisant et al., 1997, Weed et al., 2005). The ectasia results in a myopic and astigmatic refractive error significantly affecting the vision.

Fig. 1: Ectatic eye with corneal placido ring reflection, white light illumination.

The different distribution and reduction in the amount of collagen lamellae, as well as a decomposition of fibroblasts (Sherwin and Brookes, 2004) in patients suffering from keratoconus, could be regarded as a preliminary stage in the pathogenesis of keratoconus (Meek et al., 2005, Klintworth and Damms, 1995). Confocal microscopy shows a reduction of keratinocytes: the more the disease progresses, the greater the loss of keratinocytes (Ku et al., 2008). Meek et al showed by means of X-ray structure analysis that the structure of the collagen fibres changes.

This could be facilitated by a loss of cohesive forces (Meek et al., 2005). Morishige et al captured high-resolution three-dimensional images of collagen lamellae by "second harmonic imaging" (Morishige et al., 2007). It was noticeable that in healthy corneas the collagen lamellae were heavily intertwined in the anterior stroma and anchored in the Bowman layer.

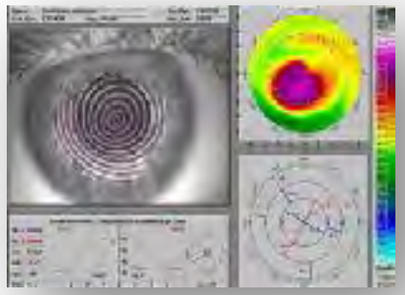

Fig. 2: Video-topograph output of an keratoconic eye (grade 2-3) .

Recent studies have assessed the difference between keratoconic and healthy corneas and the effectiveness of measuring biomechanical properties to determine the risk of keratoconus (Barbara and Rabinowitz, 2011). The biomechanical behaviour changes in keratoconic eyes, with matched IOPcc, by means of the CorvisST have been investigated, Table1. The differences identified seem to be predominantly due to variation in corneal elastic properties between normal and keratoconic corneas.

Commercial relation: none

Daniela Oehring
Plymouth University
Email: daniela.oehring@plymouth.ac.uk

Contact details

Table1: Biomechanical properties change in keratoconic eyes (Barbara and Rabinowitz, 2011)

Parameter	Keratoconic eyes in comparison to healthy eyes
Stiffness	Decrease
Corneal thickness	Decrease
Velocity	Decrease (initiate deformation earlier, but recover slower)
Applanation lengths	Decrease
Highest concavity	Steeper
Displacement at depth	Greater
Deformation depths	Greater

Purpose

Purpose of this study is to evaluate the ocular biomechanics at nine different areas across the cornea in-vivo in advanced keratoconic eyes before and after crosslinking procedure.

This preliminary analysis aimed to a descriptive overview of the first ten participants before crosslinking procedure. The CorvisST measurements were to evaluate the regional variation across the cornea of newly developed biomechanical parameters for in-vivo analysis.

Regional variation of biomechanical properties in ectatic eyes (preliminary results)

Daniela Oehring[1], Nabil Habib[2], Hetal Buckhurst[1]

1 Eye and Vision Research Group, School of Health and Human Sciences, Plymouth University, Plymouth, UK; 2 School of Optometry & Vision Sciences, Cardiff University, UK

Corneal biomechanics was assessed in 10 subjects with diagnosed keratoconus (grade 3) aged between 18-31 years (25.2±3.1); 80% female, 20% male) with the CorvisST. Only one eye was chosen randomly for the preliminary analysis (ratio 1:1).

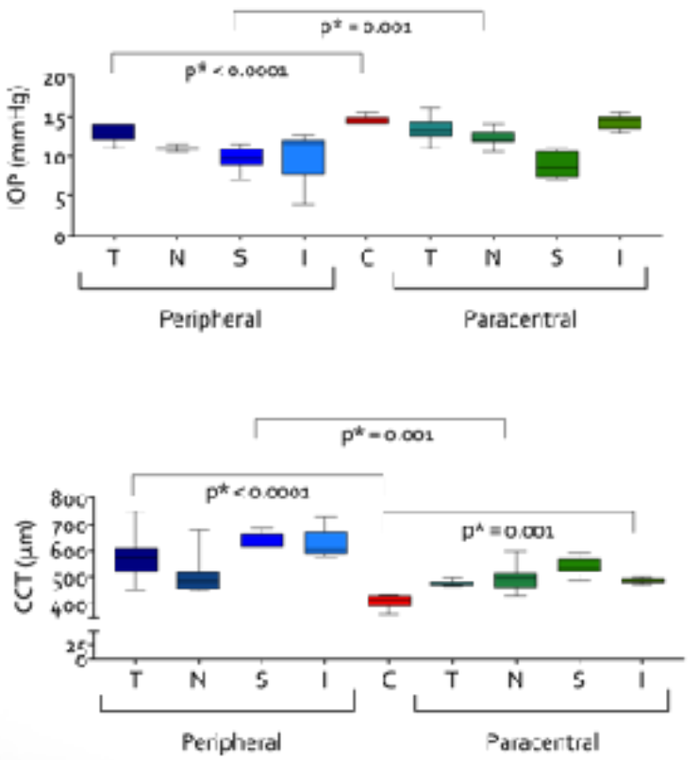

Fig. 3: Distribution of IOP (top) and CCT (bottom) for n+10 eyes in all positions. In both parameter the different zones (peripheral, paracentral and central) are significant different (Wilcoxon rank sum test, p* adjusted p-value FDR). Within the peripheral zone only CCT is significant different between T & S, T & I as well as N & S and N & I.

Methods

The movie of each single measurement was imported into Mat Lab. Consecutively, the anterior as well as the posterior surface and were tracked, in order to derive a displacement matrix (equation 1).

$$L_{CST} = \overrightarrow{d(t,c)} = \begin{bmatrix} \vec{d}_{1m} \\ \vec{d}_{2m} \\ \vec{d}_{3m} \\ \vec{d}_{4m} \\ \dots \\ \vec{d}_{nm} \end{bmatrix} = \begin{array}{c|cccccc} & c_1 & c_2 & c_3 & c_4 & \dots & c_m \\ t_1 & d_{11}(t_1c_1) & d_{12}(t_1c_2) & d_{13}(t_1c_3) & d_{14}(t_1c_4) & \dots & d_{1m}(t_2c_m) \\ t_2 & d_{21}(t_2c_1) & d_{22}(t_2c_2) & d_{23}(t_2c_3) & d_{24}(t_2c_4) & \dots & d_{2m}(t_2c_m) \\ t_3 & d_{31}(t_3c_1) & d_{32}(t_3c_2) & d_{33}(t_3c_3) & d_{34}(t_3c_4) & \dots & d_{3m}(t_3c_m) \\ t_4 & d_{41}(t_4c_1) & d_{42}(t_4c_2) & d_{43}(t_4c_3) & d_{44}(t_4c_4) & \dots & d_{4m}(t_4c_m) \\ \dots & & & & & & \\ t_n & d_{n1}(t_nc_1) & d_{n2}(t_nc_2) & d_{n3}(t_nc_3) & d_{n4}(t_nc_4) & \dots & d_{nm}(t_nc_m) \end{array}$$

Equation 1: Corneal deformation matrix $L_{CST}(c,t,d)$ (d is defined as the depth of the corneal surface at c over time (t), c describes the horizontal offset where c_0 is defined as the corneal centre).

Based on the displacement matrix for the anterior and posterior surface novel in-vivo biomechanical parameters were calculated:

- Corneal hysteresis: The magnitude of the hysteresis is equivalent to the difference between the compression during the load and unload at each specific pressure. The higher the hysteresis, the higher the difference between the compression behaviour during inward and outward movement. It characterises the dependency of the unload (outward) movement from the load (inward) movement and is material depended.
- Damping: The ratio between loss of energy and stored energy is called damping. The smaller D, the less damped is the system.
- Dynamic Young's modulus: The modulus of elasticity describes the material resistance against deformation. The higher the E-Modulus, the more pressure has to be applied to deform the material by the same amount.

Regional measurements:
To assess regional variation of biomechanical properties across the cornea a dynamic fixation target was developed (Figure 4).

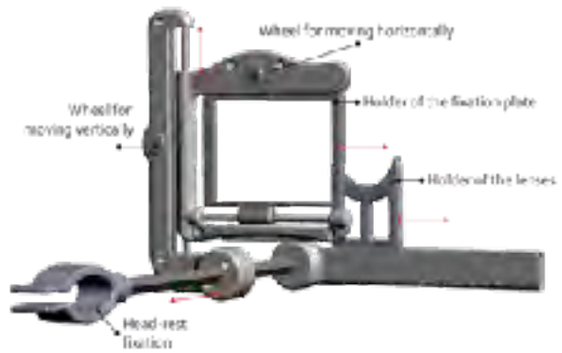

Using a semi-transparent digital display nine different position (Figure 5 bottom) across the corneal meridians (horizontally and vertically, Figure 5 top) were assesses using CorvisST.

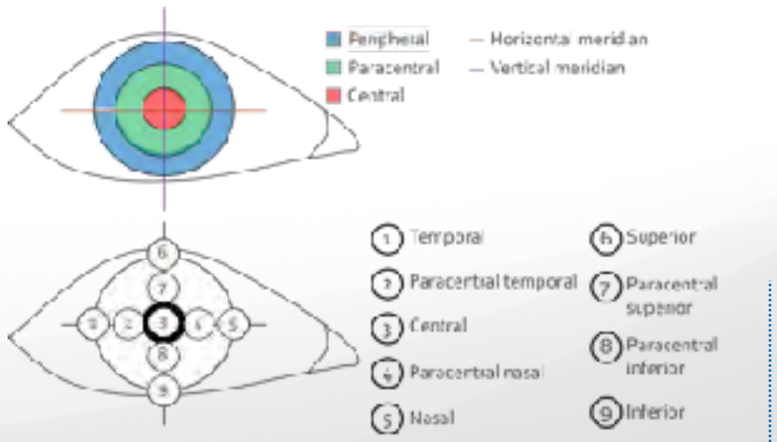

Regional variation of biomechanical properties in ectatic eyes (preliminary results)

Daniela Oehring[1], Nabil Habib[2], Hetal Buckhurst[1]
1 Eye and Vision Research Group, School of Health and Human Sciences, Plymouth University, Plymouth, UK; 2 School of Optometry & Vision Sciences, Cardiff University, UK

Results (corneal deflection)

Examples of exported movies of the CorvisST measurements (ID 008, female, KC grade 3 OD).
3D graph of the average corneal displacement centrally (n=10). The initial corneal curvature as well as whole eye movement component were eliminated from the corneal deflection matrix, thus the pure inverse corneal deflection is visible.

Peripheral corneal regions:

Horizontal meridian

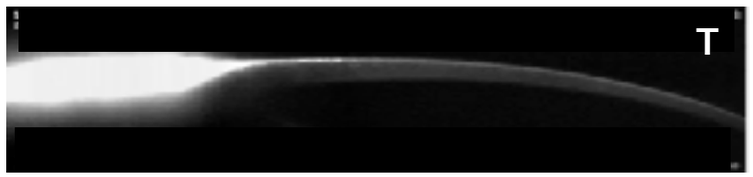

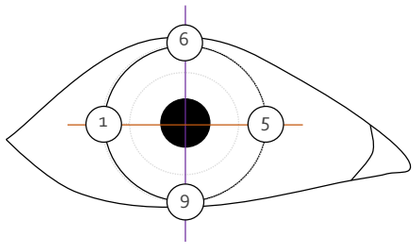

(1) (T) Temporal — Horizontal meridian
(5) (N) Nasal — Vertical meridian
(6) (S) Superior
(9) (I) Inferior

Vertical meridian

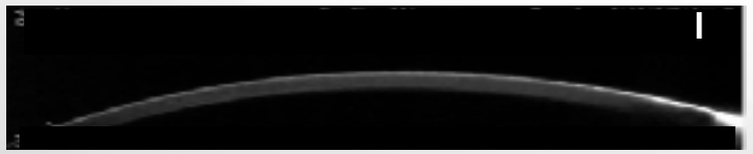

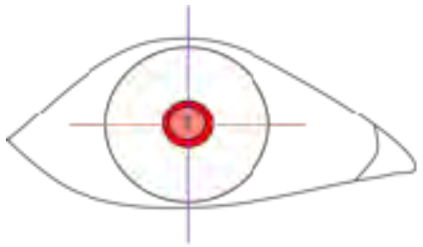

(3) (C) Central — Horizontal meridian
Vertical meridian

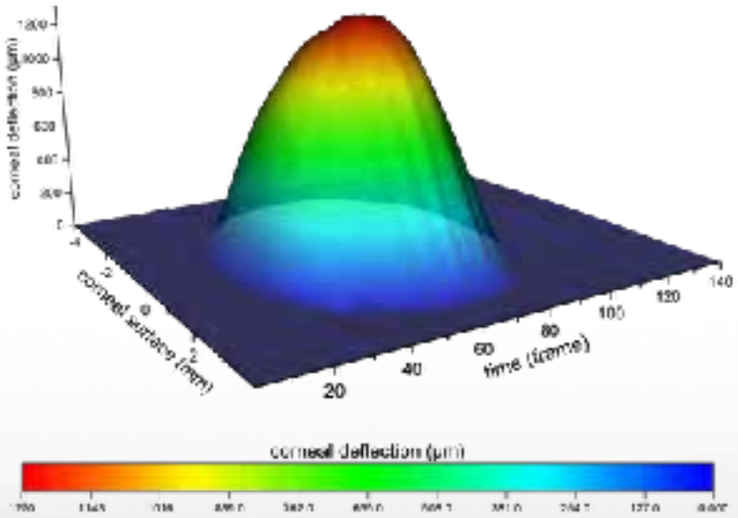

Paracentral corneal regions:

Horizontal meridian

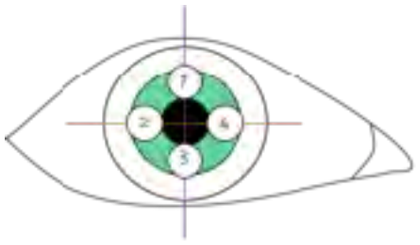

(1) (T) Temporal — Horizontal meridian
(5) (N) Nasal — Vertical meridian
(6) (S) Superior
(9) (I) Inferior

Vertical meridian

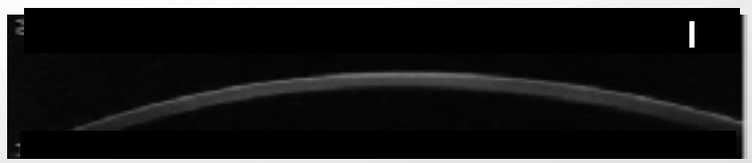

Regional variation of biomechanical properties in ectatic eyes (preliminary results)

Daniela Oehring[1], Nabil Habib[2], Hetal Buckhurst[1]

1 Eye and Vision Research Group, School of Health and Human Sciences, Plymouth University, Plymouth, UK; 2 School of Optometry & Vision Sciences, Cardiff University, UK

Deflection amplitude:

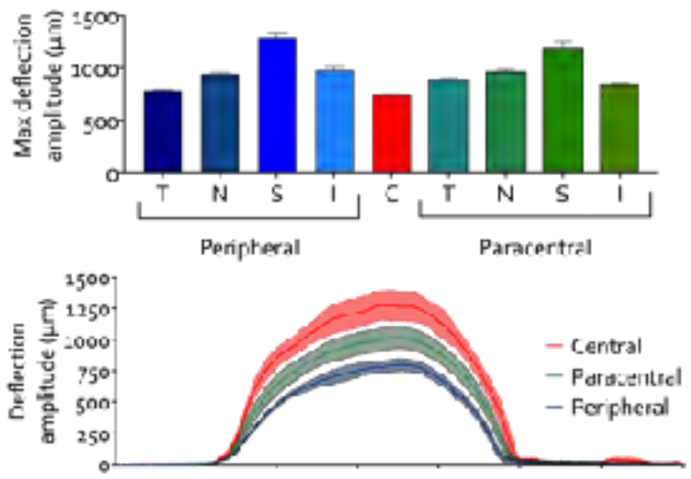

Fig. 10: Distribution of the deflection amplitude. Top: maximal deflection amplitude per position. Bottom: Deflection amplitude over time, position grouped in zones.

Applanation length:

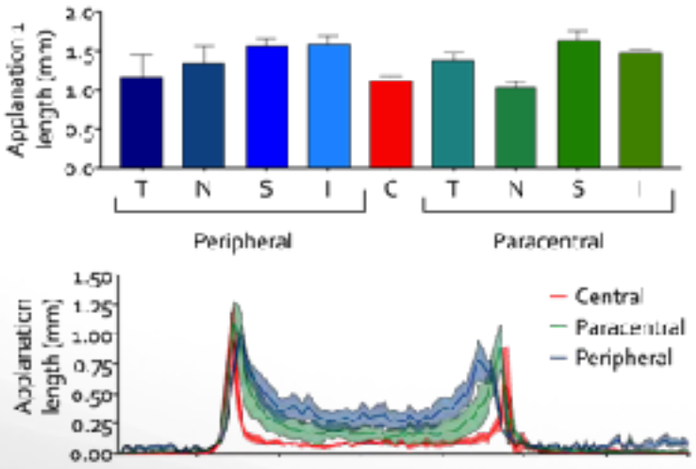

Fig. 11: Distribution of the applanation length. Top: Length at applanation 1 per position. Bottom: Applanation length over time, position grouped in zones.

Results (corneal deflection)

3D graph of the average corneal displacement per zone (n=10).

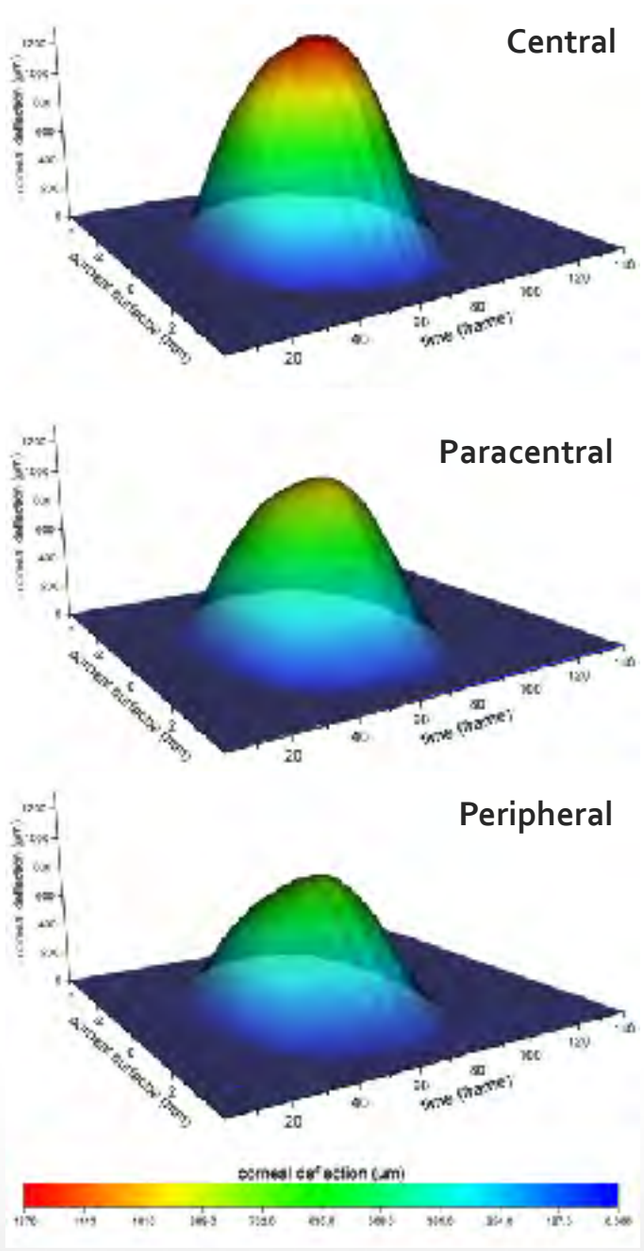

Normalised deflection (referred to centre):

Paracentral

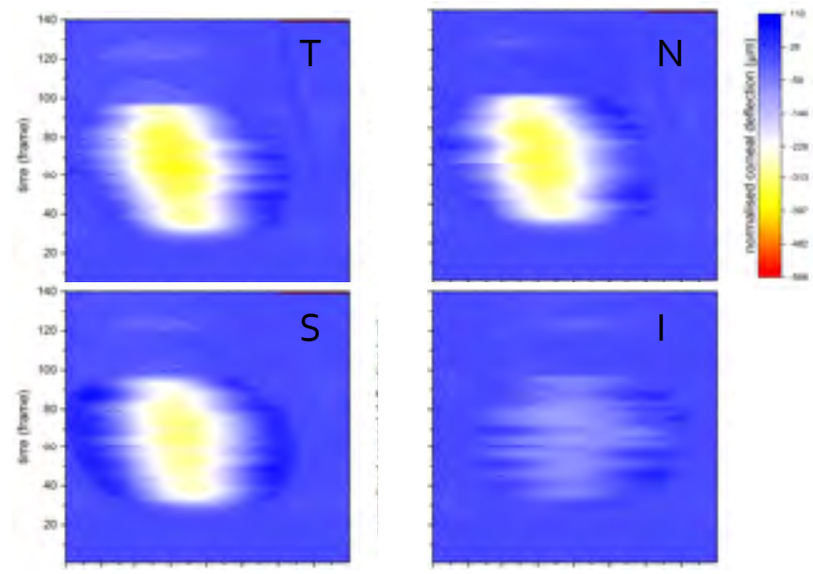

Peripheral

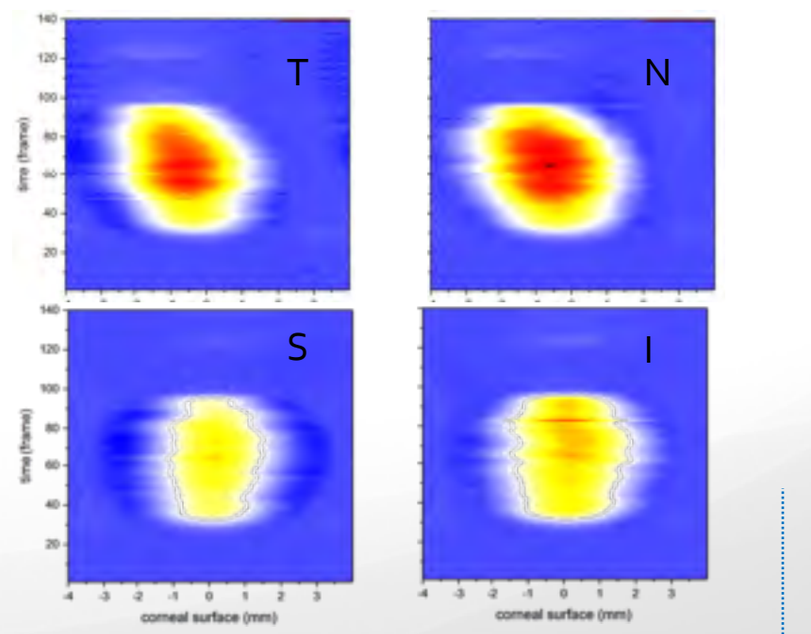

Regional variation of biomechanical properties in ectatic eyes (preliminary results)

Daniela Oehring[1], Nabil Habib[2], Hetal Buckhurst[1]
1 Eye and Vision Research Group, School of Health and Human Sciences, Plymouth University, Plymouth, UK; 2 School of Optometry & Vision Sciences, Cardiff University, UK

Results (biomechanics)

Hysteresis

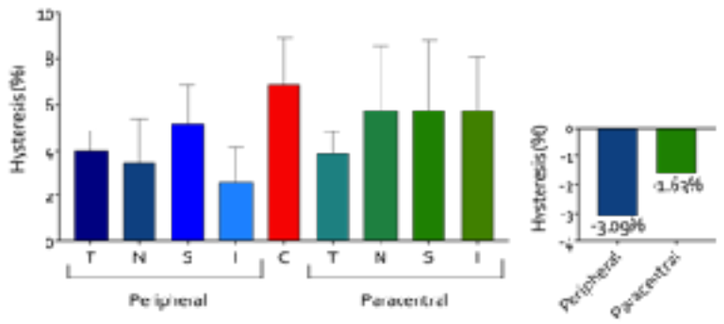

Fig. 15: Distribution of the corneal hysteresis at different position across the cornea (values see table below). Left: Absolut hysteresis grouped in peripheral (blue), central (red) and paracentral (green) locations. Right: Normalised hysteresis per zones

Position	Mean (SD) in %			
Central	6.90 (2.82)			
	T	N	S	I
Peripheral	4.02 (1.15)	3.45 (2.65)	5.17 (2.39)	2.59 (2.18)
Paracentral	3.83 (1.33)	5.75 (3.98)	5.75 (4.30)	5.75 (3.25)

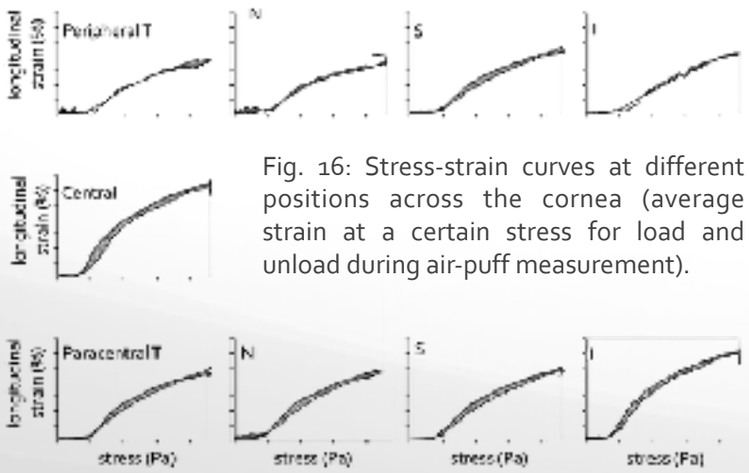

Fig. 16: Stress-strain curves at different positions across the cornea (average strain at a certain stress for load and unload during air-puff measurement).

Dynamic Young's modulus:

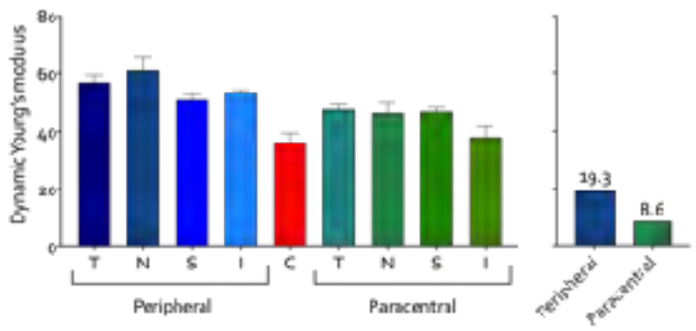

Fig. 17: Distribution of the dynamic Young's modulus at different position across the cornea (values see table below). Left: Absolut modulus grouped in peripheral (blue), central (red) and paracentral (green) locations. Right: Normalised averaged modulus per zones

Position	Mean (SD) in %			
Central	36.3 (4.5)			
	T	N	S	I
Peripheral	57.0 (3.3)	60.9 (6.9)	50.9 (2.7)	53.5 (1.3)
Paracentral	47.9 (2.1)	46.7 (4.6)	47.1 (1.9)	38.1 (5.1)

Damping

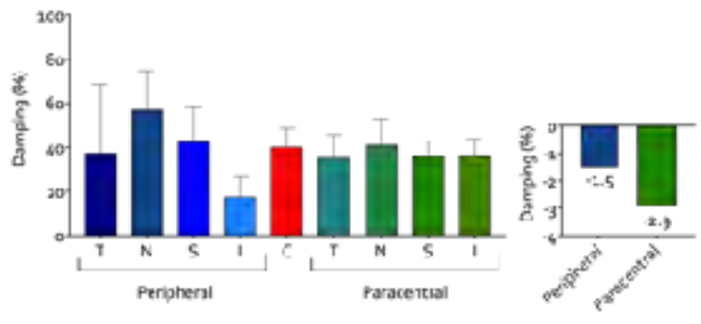

Fig. 18: Distribution of the damping at different position across the cornea (values see table below). Left: Absolut damping grouped in peripheral (blue), central (red) and paracentral (green) locations. Right: Normalised averaged damping per zones

Position	Mean (SD) in %			
Central	36.3 (4.5)			
	T	N	S	I
Peripheral	37.5 (43.4)	56.9 (25.0)	42.5 (21.6)	17.4 (12.8)
Paracentral	35.1 (1.7)	41.1 (16.5)	35.9 (9.8)	26.6 (10.0)

Conclusion

The preliminary analysis showed that in-vivo material dependent parameter could be determined using conventional NCT air-puff measurements in ectatic eyes. Furthermore it is possible to assess the biomechanics in-vivo. The preliminary analysis supports earlier findings that the farther away from the apex the cornea is becoming stiffer and more resistant against deformation.

Key references

BARBARA, A. & RABINOWITZ, Y. S. 2011. Textbook on Keratoconus: New Insights, Jaypee Brothers, Medical Publishers.
KLINTWORTH, G. K. & DAMMS, T. 1995. Corneal dystrophies and keratoconus. *Curr Opin Ophthalmol,* 6**,** 44-56.
MEEK, K. M., TUFT, S. J., HUANG, Y., GILL, P. S., HAYES, S., NEWTON, R. H. & BRON, A. J. 2005. Changes in collagen orientation and distribution in keratoconus corneas. Invest Ophthalmol Vis Sci, 46, 1948-56.

Complete list can be send by author